PHYSICAL REVIEW D VOLUME 27, NUMBER 1 1 JANUARY 1983

Z^0 decay into two gluons and a photon for massive quarks

Morten L. Laursen, Mark A. Samuel, Gary B. Tupper, and Achin Sen
Department of Physics, Oklahoma State University, Stillwater, Oklahoma 74078
(Received 26 July 1982)

We have determined the decay rates for the rare decays $Z^0 \to gg\gamma$ (ggg) including quark masses. We find a coherence effect in the amplitude for these processes which is sensitive to the top-quark mass. Inclusion of a top-quark mass of $m_t = 20$ GeV decreases the rate for $Z^0 \to gg\gamma$ by a factor of 2 and enhances the rate for $Z^0 \to ggg$ by a factor of 3. The branching ratios are $\Gamma(Z^0 \to gg\gamma)/\Gamma_0 = 1.8 \times 10^{-6}$ and $\Gamma(Z^0 \to ggg)/\Gamma_0 > 0.8 \times 10^{-5}$, where the latter is a lower bound since the axial-vector contribution has yet to be computed, and Γ_0 is the total hadronic decay width.

I. INTRODUCTION

The study of the Z^0 boson through its decays into two and three jets is of immediate interest due to the fact that the new electron-position colliders will be able to produce a substantial number of Z^0's in the near future.[1]

The rare decays $Z^0 \to gg\gamma$ and $Z^0 \to ggg$ offer an interesting way of testing the standard model of electroweak and strong interactions in higher-order perturbation theory. The differential as well as the total decay rates for these processes have been calculated via the box graph, with all the quark masses in the loop set to zero.[2]

In this paper, we extend these calculations by including the dependence on the quark masses. For the present, we shall mainly concentrate on the process $Z^0 \to gg\gamma$, because the axial-vector coupling is not involved. For the process $Z^0 \to ggg$ we shall report on the vector part only. A later paper will deal with the axial-vector part also.[3]

Our analysis shows that for a single quark flavor the total decay rate does not change substantially except near the limit $\rho = (2m_q/M_Z)^2 \to 1$ (i.e., close to the threshold for producing a $q\bar{q}$ pair). As expected, we also find a discontinuity in the slope of the decay rate at the point $\rho = 1$. The single- and double-differential rates are found to be more sensitive to the quark masses. A useful approximation, enabling us to study the quark-mass dependence of various functions, as well as reducing the computational time, has been found by setting all the five quark masses (up to the bottom) equal to m_u and by treating the top-quark mass m_t as a free parameter.

In Sec. II, we present some of the details of our calculations. Section III is devoted to our numerical results for a single-quark contribution. In Sec. IV we discuss the total contribution, including all six quarks in the loop. Since the top-quark mass is unknown, we present our results as a function of the mass of the top quark. Finally, in Sec. V, we present our conclusion.

II. DETAILS OF THE CALCULATIONS

To investigate the decay $Z^0 \to gg\gamma$ we only have to consider the box diagrams shown in Fig. 1. Owing to the symmetry in the color indices $[Tr(T_a T_b) = \frac{1}{2}\delta_{a,b}]$ only the vector couplings of the Z^0 to $q_i\bar{q}_i$ have to be included. For the other decay $Z^0 \to ggg$ (see Fig. 2) the axial-vector couplings also contribute. In the limit of vanishing quark masses this was not the case, since the contribution within each doublet would cancel. Since the contributions from the vector and axial-vector parts add incoherently we can establish a lower bound on the rate for $Z^0 \to ggg$.

After averaging over the initial spins and summing over the helicities the double-differential decay rate for $Z^0 \to gg\gamma$ can be expressed as

$$\frac{1}{\Gamma_0}\frac{d^2\Gamma(Z^0 \to gg\gamma)}{dx\,dy} = \frac{1}{256}\left[\frac{\alpha_s}{\pi}\right]^2\left[\frac{\alpha}{\pi}\right]\frac{C^{gg\gamma}}{2!} \times \frac{\left[\sum_i a_i q_i\right]^2}{\sum_i (a_i{}^2 + b_i{}^2)}\frac{d^2F}{dx\,dy} \tag{1}$$

We have of course normalized to the total hadronic

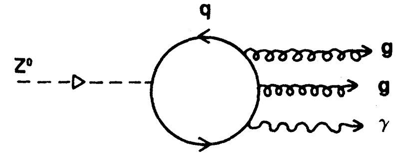

FIG. 1. Feynman diagrams for the decay $Z^0 \to gg\gamma$.

decay width:

$$\Gamma_0=\sum_i \Gamma(Z^0\to q_i\bar{q}_i)=\frac{M_Z{}^3G_F}{2\sqrt{2}\pi}\sum_i (a_i{}^2+b_i{}^2)\ . \tag{2}$$

Here q_i is the electric charge of quark i and $C^{gg\gamma}=8$ is a color factor. a_i and b_i are the usual vector and axial-vector couplings of Z^0 to $q_i\bar{q}_i$,

$$a^u=a^c=a^t=\tfrac{1}{2}-\tfrac{4}{3}\sin^2\theta_W\ ,$$

$$a^d=a^s=a^b=-\tfrac{1}{2}+\tfrac{2}{3}\sin^2\theta_W\ ,$$

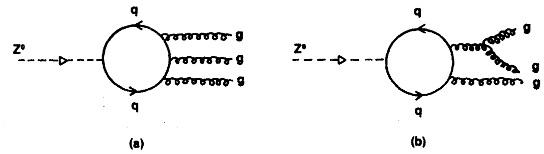

FIG. 2. Feynman diagrams for the decay $Z^0\to ggg$.

$$b^u=-b^d=b^c=-b^s=b^t=-b^b=\tfrac{1}{2}\ .$$

x and y are the usual scaling variables $x=2E_a/M_z$ and $y=2E_b/M_Z$.

The function $d^2F/dx\,dy$ is given by

$$\frac{d^2F}{dx\,dy}=\frac{16}{3}\sum_{\lambda=\pm}\Bigg\{\frac{y(1-y)}{x(1-x)}\,|\hat{E}^{(1)}_{\lambda++}(x,y,z)|^2+\frac{z(1-z)}{x(1-x)}\,|\hat{E}^{(1)}_{\lambda++}(x,z,y)|^2$$
$$-\frac{2(1-y)(1-z)}{x(1-x)}\,\mathrm{Re}[\hat{E}^{(1)}_{\lambda++}(x,y,z)\hat{E}^{(1)*}_{\lambda++}(x,z,y)]$$
$$+|\hat{E}^{(2)}_{\lambda++}(x,y,z)|^2+(x\leftrightarrow y)+(x\leftrightarrow z)\Bigg\} \tag{3}$$

with

$$\hat{E}^{(1,2)}_{\lambda++}(x,y,z)=\frac{1}{\sum_i a_iq_i}\sum_i a_iq_i\hat{E}^{(1,2)}_{\lambda++}(x,y,z,\rho_i)\ .$$

The $\hat{E}^{(i)}$'s are helicity amplitudes.[4] They are no longer real, as was the case in the limit of massless quarks. The expressions for $\hat{E}^{(1,2)}_{\lambda++}$ are much more complicated now and they are given in the Appendix. We verified explicitly that $d^2F/dx\,dy$ is free of any mass singularities; that is, no $1/(1-x)$ or $1/x$ terms are present in the limit $x\to 1$ or $x\to 0$. This serves as a check on the calculation. We also notice that $d^2F/dx\,dy$ no longer behaves like $\ln^2(1-x)$ for $x\to 1$ but rather tends to a constant. This is due to the parameter ρ_i which cuts off the logarithmic behavior near the edges of the phase space.

III. RESULTS FOR A SINGLE-QUARK CONTRIBUTION

As mentioned before, $d^2F/dx\,dy$ is free of any mass singularities and we can safely integrate to obtain the single-differential rate dF/dx and the total rate $F(\rho)$ as a function of ρ. For $\rho\to 0$ we should reproduce the answer $F(0)\simeq 80$. The other limit $\rho\to 1$ corresponds to closing the channel for the real decay $Z^0\to q\bar{q}$. A plot of $F(\rho)$ vs $\sqrt{\rho}(\rho<1)$ is exhibited in Fig. 3—it shows a very small rise up to $\rho\lesssim 0.1$ and as we reach $\rho\to 1$ the limited phase space cuts $F(\rho)$ severely. At $\rho=1$ the value of F is roughly one-third of $F(0)$. Figure 4 shows the behavior of $F(\rho)$ for $\rho>1$. For ρ values between 10 and 100 it approaches the asymptotic expression

$$F(\rho)\simeq\frac{4352}{30\,375}\frac{1}{\rho^4}$$

(easily obtained by using the asymptotic values for $\hat{E}^{(1,2)}_{\lambda++}$). As ρ approaches 1 from above, this approximation fails badly, roughly by two orders of magnitude. When the two curves are matched at

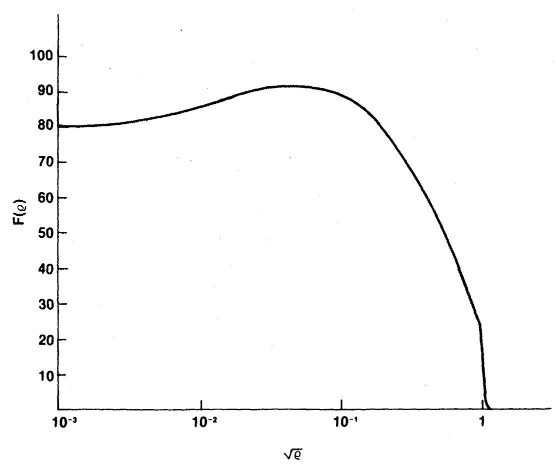

FIG. 3. The function $F(\rho)$ vs $\sqrt{\rho}$ for $\rho\leq 1$ (one quark flavor).

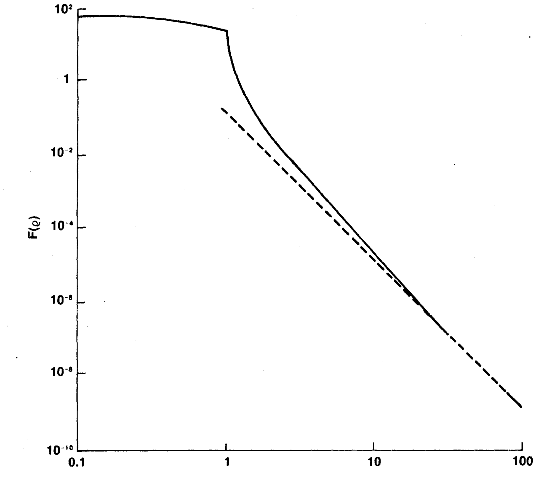

FIG. 4. The function $F(\rho)$ vs $\sqrt{\rho}$ for $\rho \geq 1$ (one quark flavor).

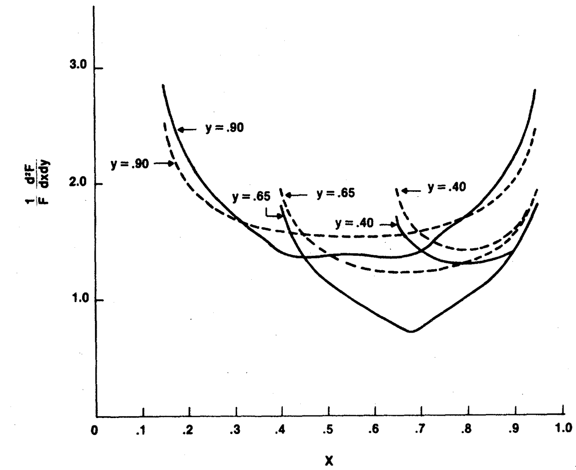

FIG. 6. The double-differential function $(1/F)d^2F/dx\,dy$ for several values of y. Solid curve includes quark masses with $\rho_t = 0.309$. Dashed curve is the massless case.

$\rho = 1$ we find a discontinuity in the slope. This of course is expected since for $\rho > 1$ the amplitudes are real functions while for $1 \geq \rho \geq 0$ they have an imaginary part. A similar discontinuity was seen before

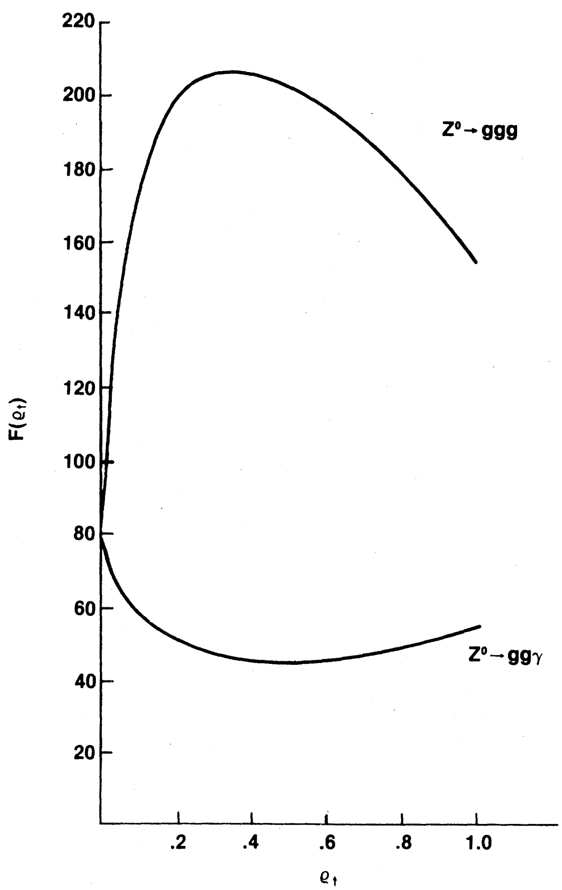

FIG. 5. The function $F(\rho_t)$ vs $\sqrt{\rho_t}$ for both processes (all six quark flavors included).

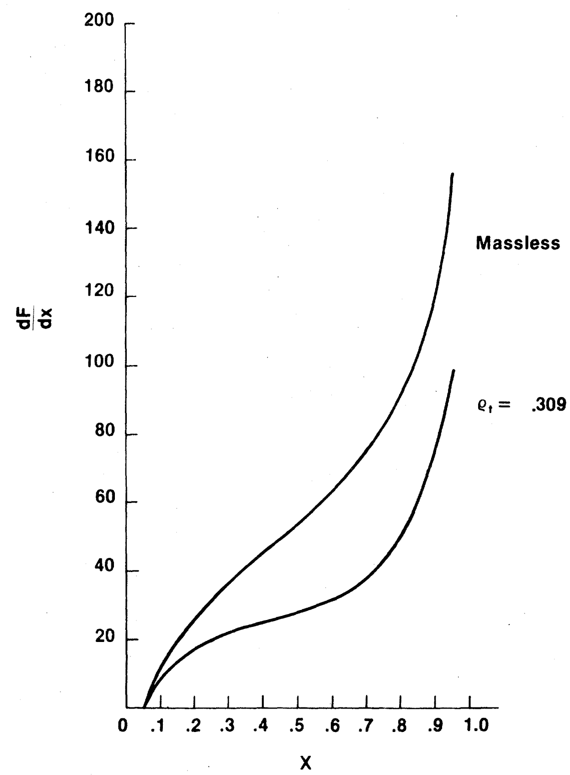

FIG. 7. The single-differential function dF/dx as a function of x. The upper curve is the massless case; the lower curve includes quark masses. A cut $\epsilon = 0.025$ is used in the massless case.

by De Tollis in the photon-photon scattering process.

For $\rho \leq 1$ our results for $F(\rho)$ are in agreement with Baier *et al.*[5]

IV. RESULTS FOR THE TOTAL CONTRIBUTION: DEPENDENCE ON THE MASS OF THE TOP QUARK

To get the total rate for $Z^0 \to gg\gamma$ one has to take into account the coherent contribution of all six quarks in the loop in Fig. 1. In most of the region of the phase space $\hat{E}^{(1,2)}_{+++}$ tends to be much larger than $\hat{E}^{(1,2)}_{-++}$. Also $\hat{E}^{(1,2)}_{\lambda++}(\rho)$ only deviates about 10% even for the bottom quark from its value at $\rho=0$, except close to the edges of the phase space. Anyway the contribution to $F(\rho)$ here is small due to the cutoff.

We then found it reasonable to use just one $\rho_i=\rho_u$ for $i=u$, d, s, c, and b. The top quark mass is treated separately and we have used it as a free parameter. A plot of $F(\rho_t)$ for $Z^0 \to gg\gamma$ as well as the vector part for $Z^0 \to ggg$ is shown in Fig. 5. For small ρ_t the value $F(0) \simeq 80$ is obtained. For $\rho_t=1$ only five quarks should contribute and F goes down to about 70% for the $Z^0 \to gg\gamma$ decay and up to about 200% in the other case. The behavior of $F(\rho_t)$ can qualitatively be understood by looking at the interference patterns in $\hat{E}^{(1,2)}_{\lambda++}$. For the process $Z^0 \to gg\gamma$ all the couplings $a_i q_i$ are positive. Also $\hat{E}^{(1,2)}_{\lambda++}(\rho_i)$ is negative for small ρ_i in most of the phase space. However, if ρ_i becomes large like ρ_t, the amplitude changes sign, thus introducing destructive interference. For the process $Z^0 \to ggg$ the opposite is the case. Here the couplings are only a_i. Since a_t is positive, a positive value of $\hat{E}_{\lambda++}$ will increase the total amplitude.

For a top-quark mass of $m_t=20$ GeV we obtain[6] the branching ratios

$$\frac{\Gamma(Z^0 \to gg\gamma)}{\Gamma_0}=1.8\times 10^{-6}$$

and

$$\frac{\Gamma(Z^0 \to ggg)}{\Gamma_0}=0.8\times 10^{-5} .$$

In Fig. 6 we also show the double differential function $d^2F/dx\,dy$ normalized to $F(\rho_t)$ compared to the massless case. Although the shape has changed we still have the symmetries around $x=1-\frac{1}{2}y$ satisfied. Finally in Fig. 7 we have displayed the single-differential function dF/dx and compared it with the massless case. For small x they give the same answer, while for $x \to 1$, $dF(\rho_t)/dx$ tends to a finite value and $dF(0)/dx$ goes like $\ln^2(1-x)$.

V. REMARKS AND CONCLUSIONS

(a) Our results are based on the assumption that the gluon jets are indistinguishable, because we are below the color threshold. Above the color threshold the results for $Z^0 \to gg\gamma$ and $Z^0 \to ggg$ should be multiplied by a factor 2! and 3!, respectively.

(b) The plot of the function $F(\rho)$ vs $\sqrt{\rho}$ (see Fig. 3) is identical in shape to a similar plot exhibited by Baier *et al.* However we found a discontinuity in the slope of $F(\rho)$ at $\rho=1$.

(c) We have seen that for the process $Z^0 \to ggg$ the rate increases almost by a factor of 3. This is encouraging, since this would suggest that the axial-vector part also could give a reasonable contribution, thus maybe increasing the rate even further.

Note added in proof. A very interesting paper by F. M. Renard has recently been published,[7] in which it is pointed out that the rare decays $Z^0 \to ggg$, $Z^0 \to gg\gamma$, and $Z^0 \to \gamma\gamma\gamma$ can be used as sensitive tests of any Z^0 compositeness. That is, if the Z^0 is a composite object, the rates for these decays will be substantially larger than the standard-model results presented here.

ACKNOWLEDGMENTS

It is a pleasure to thank G. P. Lepage, J. P. Leveille, K. O. Mikaelian, and K. Milton for valuable discussions. This work was supported by the U. S. Department of Energy under Contract No. EY-76-S-05-5074.

APPENDIX

Let $r=1-x$, $s=1-y$, and $t=1-z$. The helicity amplitudes now read

$$\hat{E}^{(1)}_{+++}(x,y,z)=\frac{2t}{1-s}+\left[\frac{4st}{r(1-s)}+\frac{4t}{(1-s)^2}-\frac{2s}{1-s}\right]\left[B\left[\frac{s}{\rho}\right]-B\left[\frac{1}{\rho}\right]\right]$$
$$+\left[\frac{4t}{r}+\frac{2t}{1-t}\right]\left[B\left[\frac{t}{\rho}\right]-B\left[\frac{1}{\rho}\right]\right]+\left[\frac{\rho}{r}-\frac{\rho}{t}\right]T\left[\frac{r}{\rho}\right]$$

$$+\left[\frac{2(s-t)}{r}-\frac{4st}{r^2}+\frac{3\rho}{1-s}-\frac{2\rho t}{(1-s)^2}-\frac{\rho}{r}-\frac{\rho}{t}-\frac{\rho}{s}\right]T\left[\frac{s}{\rho}\right]$$

$$+\left[\frac{2(s-t)}{r}-\frac{4st}{r^2}-\frac{\rho}{1-t}-\frac{\rho}{r}\right]T\left[\frac{t}{\rho}\right]$$

$$+\left[-\frac{2(s-t)}{r}+\frac{4st}{r^2}-\frac{3\rho}{1-s}+\frac{\rho}{1-t}+\frac{2\rho t}{(1-s)^2}+\frac{\rho}{r}+\frac{\rho}{t}\right]T\left[\frac{1}{\rho}\right]$$

$$+\frac{\rho(1-r)(r-t)}{rst}I_0\left[\frac{r}{\rho},\frac{s}{\rho},\frac{1}{\rho}\right]-\frac{\rho(1-r)}{rt}I_0\left[\frac{r}{\rho},\frac{t}{\rho},\frac{1}{\rho}\right]$$

$$+\left[-\frac{2(s-t)}{r}+\frac{4st}{r^2}-\frac{\rho}{t}+\frac{3\rho}{r}+\frac{2\rho}{s}\right]I_0\left[\frac{s}{\rho},\frac{t}{\rho},\frac{1}{\rho}\right],$$

$$\hat{E}^{(1)}_{-++}(x,y,z)=\left[\frac{\rho}{t}-\frac{\rho}{r}\right]\left[T\left[\frac{r}{\rho}\right]+(r\leftrightarrow s)+(r\leftrightarrow t)-(r\rightarrow 1)\right]-\left[\frac{\rho(1-r)}{st}I_0\left[\frac{r}{\rho},\frac{s}{\rho},\frac{1}{\rho}\right]-(r\leftrightarrow t)\right],$$

$$\hat{E}^{(2)}_{+++}(x,y,z)=\left\{\left[\frac{4s}{r}-\frac{2s}{1-s}\right]\left[B\left[\frac{s}{\rho}\right]-B\left[\frac{1}{\rho}\right]\right]+(s\leftrightarrow t)\right\}-\left[\frac{\rho}{r}+\frac{\rho}{s}+\frac{\rho}{t}\right]T\left[\frac{r}{\rho}\right]$$

$$+\left\{\left[-\frac{4st}{r^2}-\frac{2(1-r)}{r}-\frac{\rho r}{t(1-r)}-\frac{3\rho}{r}\right]T\left[\frac{s}{\rho}\right]+(s\leftrightarrow t)\right\}$$

$$+\left[\frac{4st}{r^2}+\frac{2(1-r)}{r}+\frac{\rho(1-r)}{st}-\frac{\rho}{1-s}-\frac{\rho}{1-t}+\frac{3\rho}{r}\right]T\left[\frac{1}{\rho}\right]$$

$$+\left\{\left[\frac{\rho t}{rs}+\frac{\rho(1-s)}{rt}+\frac{\rho^2}{rs}\right]I_0\left[\frac{r}{\rho},\frac{s}{\rho},\frac{1}{\rho}\right]+(s\leftrightarrow t)\right\}$$

$$+\left[\frac{4st}{r^2}+\frac{2(1-r)}{r}+\frac{\rho(1-r)}{st}+\frac{5\rho}{r}+\frac{\rho^2}{st}\right]I_0\left[\frac{s}{\rho},\frac{t}{\rho},\frac{1}{\rho}\right],$$

$$\hat{E}^{(2)}_{-++}(x,y,z)=-2-\left[\frac{\rho}{r}+\frac{\rho}{s}+\frac{\rho}{t}\right]\left[T\left[\frac{r}{\rho}\right]+(r\leftrightarrow s)+(r\leftrightarrow t)-(r\rightarrow 1)\right]$$

$$+\left[\left[\frac{\rho}{t}+\frac{\rho^2}{rs}\right]I_0\left[\frac{r}{\rho},\frac{s}{\rho},\frac{1}{\rho}\right]+(s\leftrightarrow t)+(r\leftrightarrow t)\right].$$

Here

$$B\left[\frac{r}{\rho}\right]=\begin{cases}\left[\frac{\rho}{r}-1\right]^{1/2}\arcsin\left[\left[\frac{r}{\rho}\right]^{1/2}\right]-1, & 0\le r\le\rho\,,\\ \left[1-\frac{\rho}{r}\right]^{1/2}\ln\left[\left[\frac{r}{\rho}\right]^{1/2}+\left[\frac{r-\rho}{\rho}\right]^{1/2}\right]-1-\frac{i\pi}{2}\left[1-\frac{\rho}{r}\right]^{1/2}, & \rho\le r\le 1\,,\end{cases}$$

$$T\left[\frac{r}{\rho}\right]=\begin{cases}-\left\{\arcsin\left[\left[\frac{r}{\rho}\right]^{1/2}\right]\right\}^2, & 0\le r\le\rho\,,\\ \left[\ln\left[\left[\frac{r}{\rho}\right]^{1/2}+\left[\frac{r-\rho}{\rho}\right]^{1/2}\right]\right]^2-\frac{\pi^2}{4}-i\pi\ln\left[\frac{r}{\rho}\right]^{1/2}, & \rho\le r\le 1\,;\end{cases}$$

$$I_0\left[\frac{r}{\rho},\frac{s}{\rho},\frac{1}{\rho}\right]=F\left[\frac{r}{\rho},a\right]+F\left[\frac{s}{\rho},a\right]-F\left[\frac{1}{\rho},a\right]$$

with

$$F\left[\frac{u}{\rho},a\right]=\begin{cases}\frac{1}{2a}\left[\ln\left[\frac{ut+rs}{rs}\right]\ln\left[\frac{a+1}{a-1}\right]-\mathrm{Li}_2\left[\frac{ut}{ut+rs}\right]\right.\\ \qquad\left.+4\,\mathrm{Li}_2\left[\left[1-\frac{1}{a}\right]\cos\theta,\theta\right]-2\left[\frac{\pi}{2}-\theta\right]^2\right], & 0\le u\le\rho\,,\\ \frac{1}{2a}\left\{\ln\left[\frac{ut+rs}{rs}\right]\ln\left[\frac{a+1}{a-1}\right]-\frac{2\pi^2}{3}\right.\\ \qquad+\left[\mathrm{Li}_2\left[\frac{a+b}{a+1}\right]+\mathrm{Li}_2\left[\frac{a-1}{a+b}\right]+\tfrac{1}{2}\ln^2\left[\frac{a+1}{a+b}\right]+(b\leftrightarrow -b)\right]\\ \qquad\left.+\frac{i\pi}{2a}\ln\left[\frac{a-b}{a+b}\right]\right\}, & \rho\le u\le 1\,.\end{cases}$$

Here

$$a=\left[1+\frac{\rho t}{rs}\right]^{1/2}\text{ and } b=\left[1-\frac{\rho}{u}\right]^{1/2}.$$

Finally,

$$\mathrm{Li}_2(x)=-\int_0^x\frac{\ln(1-t)}{t}\,dt$$

and

$$\mathrm{Li}_2(x,\theta)=\mathrm{Re}\,\mathrm{Li}_2(xe^{i\theta})=-\tfrac{1}{2}\int_0^x\frac{\ln(1-2t\cos\theta+t^2)}{t}\,dt,\quad \theta=\arccos\left[\frac{u}{\rho}\,\frac{rs+\rho t}{ut+rs}\right]^{1/2}.$$

---

[1] C. H. Llewellyn Smith, University of Oxford Report No. 96-81 (unpublished).

[2] M. L. Laursen, K. O. Mikaelian, and M. A. Samuel, Phys. Rev. D 23, 2795 (1981); M. L. Laursen and M. A. Samuel, Z. Phys. C 14, 325 (1982). For related work on $e^+e^-\to gg\gamma$ and ggg see B. L. Cambridge, Nucl. Phys. B174, 243 (1980); M. L. Laursen, K. O. Mikaelian, and M. A. Samuel, Phys. Rev. D 25, 710 (1982).

[3] M. L. Laursen, M. A. Samuel, A. Sen, and G. B. Tupper (work in progress).

[4] V. Costantini, B. De Tollis, and G. Pistoni, Nuovo Cimento 2A, 733 (1971); B. De Tollis, *ibid.* 32, 757 (1964); 35, 1182 (1965).

[5] V. Baier, E. Kurayev, and B. Fadin, Yad. Fiz. 31, 700 (1980) [Sov. J. Nucl. Phys. 31, 364 (1980)].

[6] We use

$$\alpha_s=12\pi/[21\ln(M_Z{}^2/\Lambda^2)]\simeq 0.17$$

and $\sin^2\theta_W=0.23$.

[7] F. M. Renard, Phys. Lett. 116B, 269 (1982).